

## MULTI-SENSOR SYSTEMS FOR LAND-BASED AND AIRBORNE MAPPING: TECHNOLOGY OF THE FUTURE?

Dorota A. Grejner-Brzezinska<sup>1</sup>, Ron Li<sup>1</sup>, Norbert Haala<sup>2</sup>, Charles Toth<sup>3</sup>

<sup>1</sup>Department of Civil and Environmental Engineering and Geodetic Science, The Ohio State University

<sup>2</sup>Institute for Photogrammetry (IFP), University of Stuttgart

<sup>3</sup>Center for Mapping, The Ohio State University

### Commission II, WG II/1

**KEY WORDS:** Navigation, Orientation, Augmented Reality, Visualisation

#### ABSTRACT:

Technological advancements in positioning/navigation and imaging sensors that occurred during the last decade of the twentieth century, practically redefined the concept of airborne and land-based mapping. The advent of first Mobile Mapping Systems in early 1990s initiated the process of establishing modern, fully digital, virtually ground control-free photogrammetry and mapping. By the end of the last decade, Mobile Mapping technology has made a remarkable progress, evolving from rather simple land-based systems to more sophisticated, real-time multi-tasking and multi-sensor systems, operational in land and airborne environments. Following the proliferation of GPS/INS integrated technology in the mid 1990s, the quality of Direct Platform Orientation reached the level of supporting even demanding airborne mapping. New, specialized systems, based on modern imaging sensors, such as CCD cameras, LIDAR and hyper/multi-spectral scanners, are being developed, aimed at automatic data acquisition for GIS databases, thematic mapping, land classification, terrain modelling, etc. This paper provides a brief overview of the Mobile Mapping concept, with a special emphasis on GPS/INS module providing direct image sensor orientation, as well as their evolution since early 1990s. A short review of the navigation concept is given, and a notion of GPS/INS integration is presented. The concept of direct georeferencing is briefly explained and compared to the traditional AT method of image geo-registration, and the importance of multi-sensor system calibration is presented, including its impact on the positioning accuracy. Finally, some examples of currently attainable navigation and mapping accuracy for various applications, and conditions under which it is achievable are discussed. Future perspectives of MMS are also presented. Some example of MMS use in automatic object recognition, real-time highway centreline mapping, thematic mapping and city modelling with LIDAR and multispectral imagery, are also presented.

### 1. INTRODUCTION

This paper is intended as a review of the mobile mapping technology, focused on the concept definition, its evolution, and the most recent advances in both direct georeferencing, which is a backbone of this technology, as well as the imaging component, and the operational aspects related to a variety of applications. The primary objective is to provide the readers with a summary review, supported by the extended references, where detail information can be found. A variety of topics are covered, starting from direct georeferencing, through the multi-sensor system concept and its calibration. Example applications in land and airborne environments are also presented. An attempt is made to present the currently achievable accuracy, point out the newest trends and challenges that the technology still faces, and to anticipate the future developments.

The concept of Mobile Mapping System (MMS) dates back to late 1980s, when the Ohio State University Center for Mapping initiated the GPSVan™ project, leading to the development of the first directly georeferenced and fully digital land-based mapping system in 1991 (Bossler et al, 1991; He and Novak, 1992; He et al, 1994, Bossler and Toth, 1995). At the same time, the University of Calgary started a joint project with GEOFIT Inc., aimed at the development of VISAT system designed for mobile highway mapping (Schwarz et al, 1993; El-Sheimy et al, 1995). By mid-1990s more systems, based on similar concept,

have been developed, among them GPSVision by Lambda Tech International, Inc (He et al, 1996). Moreover, proliferation of GPS/INS integrated technology, facilitating high accuracy direct platform orientation (DPO), enabled the development of modern airborne systems. By mid-1990s, several systems and applications based on fully digital GPS/INS-georeferenced imagery were reported, making a transition from GPS-supported aerotriangulation (AT) to virtually ground control free photogrammetry (see for example, Schwarz et al., 1993; Lithopoulos et al., 1996; Da, 1997; Grejner-Brzezinska, 1997; Toth, 1998). Subsequently, more specialized imaging sensors were included, especially in airborne mapping, among them LIDAR (Light Detection and Ranging) and multi/hyper-spectral scanners, primarily for gathering terrain and land classification data (Axelsson, 1999; Baltsavias, 1999). A list of major existing land-based mobile mapping systems, and more details on the modern sensors and airborne systems, can be found in (Grejner-Brzezinska, 2001a and 2001b).

Multi-sensor systems that combine direct positioning and imaging sensors are rapidly becoming a standard source of information for various aerial mapping applications including orthophoto production, feature extraction/vector mapping, and surface reconstruction. An optimal fusion of multi-sensory data, supported by geometric fusion facilitated by GPS/INS (Global Positioning System/Inertial Navigation System), provides complementary information, as sensors based on different

physical principles register different properties of objects. This, in turn, translates to a more consistent scene description enabling an improved scene interpretation/understanding. However, proper individual sensor calibration and inter-calibration become crucial in providing required mapping accuracy, as no provision can be made for incorrect or varying sensor inner orientation, when DPO is used. For example, the laser ranging device can deliver range information with the accuracy of below 10 cm. Thus, in order to properly utilize this high quality information, the sensor has to be positioned and oriented with a comparable accuracy. The quality and stability of calibration and time synchronization are especially important for airborne systems, where the object distance is significantly larger as compared to the land-based applications. Any error in IO (Interior Orientation), timing or boresight components would translate directly into errors in ground coordinates of the extracted objects, since, contrary to the aero triangulation (AT) process, the IO and EO (Exterior Orientation) estimation processes are decoupled (no common adjustment procedure that could compensate for imprecise IO or boresight transformation parameters). Some examples of boresight calibration (transformation between INS body frame and the image sensor frame) for CCD camera and LIDAR system are presented in the sequel.

**1.1 Major Operational Components of MMS**

Major operational components of MMS are listed below, while Table 1 presents the primary sensors used, and their functionality.

- System calibration
  - GPS/INS lever arm (offsets between the GPS antenna phase centre and the centre of the INS body frame)
  - Camera calibration
  - INS/camera boresight calibration (linear and angular offsets between INS and the camera and body frames)
- GPS/INS/image data collection
  - GPS/INS/camera time synchronization
  - Data logging
  - Image compression and storage
- GPS/INS post-processing for six exterior orientation parameters (time-tagged image registration to the navigation system positioning results)
- Image processing on a softcopy system (georeferenced images are used for feature location; for less demanding application monoscopic image processing suffice; when high accuracy is required, stereo imagery and restitution must be used)

**2. GPS/INS INTEGRATION: PRINCIPLES**

Several modern airborne digital sensors that work in a continuous scanning mode (multi/hyper-spectral scanners), or non-conventional (non-optical) imaging sensors, such as LIDAR, SAR (IFSAR), require GPS/INS for direct georeferencing. However, for analog or digital area-based sensors, direct georeferencing, although not compulsory, still brings obvious economic benefits by largely eliminating the need for the most complex task of photogrammetry – aerotriangulation. Consequently, multi-sensor data fusion has

become a crucial step in the design of a mobile mapping system (especially airborne), and spatial data processing algorithms. The fundamental step of any data integration process is time-space registration also called geometric fusion, most commonly provided by GPS/INS. For example, LIDAR or RADAR systems need accurate platform motion data; otherwise, the high-accuracy potential of the range data cannot be realized. Since these sensors work with rather high data transmission frequencies (10 kHz or higher), typically, the platform positioning data represent the most important term in the overall error budget. Consequently, high accuracy and reliability of DPO is crucial, therefore the issue of using an optimal navigation sensor suite is of foremost importance.

| Primary sensor   | Sensor Functionality  |
|--|---|
| <b>GPS</b>   | <ul style="list-style-type: none"> <li>• Image geo-positioning in 3D</li> <li>• Time synchronization between GPS and INS</li> <li>• Image time-tagging</li> <li>• INS error control</li> <li>• Furnishes access to the 3D mapping frame through WGS84</li> </ul>  |
| <b>INS</b>   | <ul style="list-style-type: none"> <li>• Image orientation in 3D</li> <li>• Supports image georeferencing</li> <li>• Provides bridging of GPS gaps                             <ul style="list-style-type: none"> <li>○ Provides continuous, up to 256Hz, trajectory between the GPS measurement epochs</li> </ul> </li> <li>• Supports ambiguity resolution after losses of lock, and cycle slip detection and fixing</li> </ul> |
| <b>Pseudolite Transmitter/transceiver</b>                        | <ul style="list-style-type: none"> <li>• Primary positioning functions identical to GPS</li> <li>• Supports GPS constellation during weak geometry (urban canyons)</li> </ul>   |
| <b>Camera</b>  | <ul style="list-style-type: none"> <li>• Collects imagery used to derive object position                             <ul style="list-style-type: none"> <li>○ Two (or more) cameras provide 3D coordinates in space</li> </ul> </li> </ul>  |
| <b>Laser Range Finder</b>  | <ul style="list-style-type: none"> <li>• Supports feature extraction from the imagery by providing precise distance (typical measuring accuracy is about 2-5 mm)</li> </ul>   |
| <b>LIDAR (airborne systems)</b>                                  | <ul style="list-style-type: none"> <li>• Source of DSM/DTM, also material signature for classification purposes</li> <li>• Supports feature extraction from the imagery</li> </ul>  |
| <b>Multi/hyper spectral sensors (airborne systems)</b>           | <ul style="list-style-type: none"> <li>• Spectral responses of the surface materials at each pixel location</li> <li>• Wealth of information for classification and image interpretation</li> </ul>   |
| <b>Voice recording, touch-screen, barometers, gravity gauges</b> | <ul style="list-style-type: none"> <li>• Attribute collecting sensors (land-based systems mainly)</li> </ul>  |

Table 1. Primary sensors of MMS and their functionality (partly shown in Grejner- Brzezinska, 2001a)

| Characteristics      | GPS  | INS  |
|----------------------|--|--|
| <b>Advantages</b>    | <ul style="list-style-type: none"> <li>• High accuracy of position and velocity estimation</li> <li>• Practically time-independent error spectrum</li> <li>• Attitude estimation with multiple antennas with moderate accuracy (1-2 arcmin); can be considered as a disadvantage due to rather low accuracy)</li> </ul>                            | <ul style="list-style-type: none"> <li>• Self contained and independent system</li> <li>• No gaps in data acquisition</li> <li>• Three positioning and three attitude components always available</li> <li>• High data sampling rate (up to 256 Hz)</li> </ul> |
| <b>Disadvantages</b> | <ul style="list-style-type: none"> <li>• Losses of lock causing gaps in positioning</li> <li>• Low data sampling rate (1-10 Hz)</li> <li>• Possible long ambiguity resolution time over long baseline and/or in the presence of high ambient noise</li> <li>• Moderate accuracy (1-2 arcmin) attitude estimation with multiple antennas</li> </ul> | <ul style="list-style-type: none"> <li>• Sensor error grow with time, causing positioning error divergence</li> </ul>  |

Table 2. GPS/INS summary characteristics (Grejner-Brzezinska, 2001a).

GPS and INS are navigation techniques based on entirely different positioning principles – as a radio navigation satellite system, GPS provides essentially geometric information, while autonomous INS offers inertial information, i.e., the reaction to the applied force. Consequently, these techniques offer highly complementary operational characteristics. GPS in a stand-alone mode provides a 3D position fix as long as it is able to maintain lock to a minimum of four satellites. Passive, autonomous navigation sensor, such as INS, does not require any signal reception, and its operation is virtually independent on the external conditions. Inertial navigation systems provide self-contained and independent means of 3D positioning and orientation with potentially high short-term accuracy. In addition, compared to conventional GPS output rate, INS provides much higher positioning update rates (up to 256 Hz). However, INS accuracy degrades over time due to uncompensated gyro and accelerometer errors.

Thus, full operational GPS capability, combined with steadily falling prices of medium to high-end strapdown INS, enabled an optimal combination of GPS with inertial navigation for precision mapping applications. This sensor fusion brings a number of advantages over stand-alone inertial or GPS navigation (see Table 2). GPS contributes its high accuracy and stability overtime, enabling continuous monitoring of inertial sensor errors. Implementation of closed-loop INS error calibration in Kalman filter environment allows continuous, on-the-fly error update (and thus INS calibration), leading to increased estimation accuracy. Most of the modern MMS systems rely on high-accuracy differential GPS and strapdown INS, while early systems used simpler, and lower quality dead-reckoning systems (wheel counter or odometer, directional and vertical gyros). Naturally, the accuracy strongly depends on the type of sensors used, and ranges from meters (early systems) to centimeters (new generation MMS). In general, using a GPS-calibrated, high to medium accuracy inertial system, attitude accuracy of 10-30 arcsec can be achieved (Schwarz and Wei, 1994; Abdullah, 1997; Grejner-Brzezinska, 1997; Grejner-Brzezinska and Phuyal, 1998).

GPS/INS is considered a rather settled technology, and sufficient references to the earlier publication are provided here. However, application of pseudolites (PL) in MMS is a rather new and unexplored area, therefore some preliminary results of a pilot study conducted at OSU are presented here.

**2.1 Application of Pseudo-satellites to GPS/INS Systems**

An additional sensor, which has the potential to substantially improve MMS positioning performance, especially in urban canyons, is a pseudolite (pseudo-satellite). Pseudolites are ground-based transmitters, which send a GPS-like signal to support positioning and navigation in situations where the satellite constellation may be insufficient. They are usually located

on building rooftops, high poles, or any high location in the vicinity of the survey area, which results in a relatively low elevation angle, as compared to GPS satellites. However, the signal from a low PL can strengthen the geometry of position determination, especially in the height direction. An additional GPS-like signal can also support the process of ambiguity resolution. The GPS pseudolites have been primarily used in precision landing system such as LAAS (Local Area Augmentation System) (see, for example, Barltrop et al., 1996; Hein et al., 1997), and deformation monitoring (Barnes et al., 2002; Meng et al., 2002). Recently, they have been tested in mobile mapping applications, to support weak GSP constellation in urban canyons (Wang et al., 2001; Grejner-Brzezinska et al., 2002; Lee et al., 2002).

GPS pseudolites transmit GPS-like signals on L1 (1575.42MHz) and possibly on L2 (1227.6MHz) frequencies, using C/A or P-code. GPS hardware that can accept PRN above 32 can track a pseudolite signal using an ID of 32 and above. If PRN up to 32 only can be accepted, pseudolites normally can be programmed to use a PRN currently not in use by any GPS satellite. It should be mentioned that PL signal could potentially interfere with the satellite signals due to the fact that the PL transmitter is very close to the receiving antenna, as compared to the GPS satellites (the near-far problem). Commonly used methods to overcome

these problems are: pulsing the PL signals at a fixed cycle rate, or applying a frequency offset (e.g., 1MHz from L1), or controlling the signal power. Other possible problems, associated with the use of pseudolites, are:

- due to the short distance between the receiver and the PL, any errors in the PL location will have a significant impact on the receiving antenna coordinates since PL remains stationary, its location bias is constant, and the amount of error introduced to the position coordinates of the rover receiver depends on the geometry between the PL and the receiver
- bad geometry may cause singularity in the solution; thus the location of PL must be carefully calibrated (see, for example, LeMaster and Rock, 1999)
- since PL signal travels through the base of the atmospheric layer, atmospheric models, different from those used for the GPS signal, must be applied
- due to the closeness of PL and the receiver, the PL signal is strong as compared to GPS signal; thus, possible strong multipath signature of the PL signal may come from the transmitter itself, not only the reflecting objects (helical antennas are recommended to mitigate this effect)
- due to totally different geometry as compared to GPS, differential technique (based on GPS and PL together) will eliminate fewer error sources; consequently, the PL location error or tropospheric effects will not cancel with double differences (DD), as the geometry is not identical for the mobile user and the reference station (especially for longer baselines).

Preliminary tests on using PL in mobile mapping environment were conducted at The Ohio State University in May 2001. An IN200CXL pseudolite, manufactured by IntegriNautics Inc., on loan from the University of New South Wales, was used, and two additional PL locations/signals were simulated. As an example of the impact of using PLs in GPS/INS/PL system, on the positioning accuracy, Figures 1 and 2 show the RVDOP (Relative Vertical Dilution of Precision) and number of observations for GPS-only observable (blue), GPS plus one PL (red), and GPS plus three PLs (green). Table 3 illustrates the comparison of the positioning quality between the GPS-only weak constellation (four high satellites) and the same GPS constellation, supported by three pseudolite signals at elevations ranging from 7° to 13°, located at the corners of the mapped area (Grejner-Brzezinska et al., 2002).

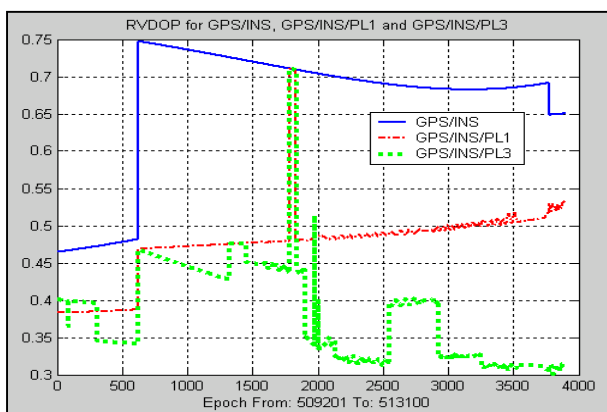


Figure 1. Relative Vertical Dilution of Precision, GPS and PLs.

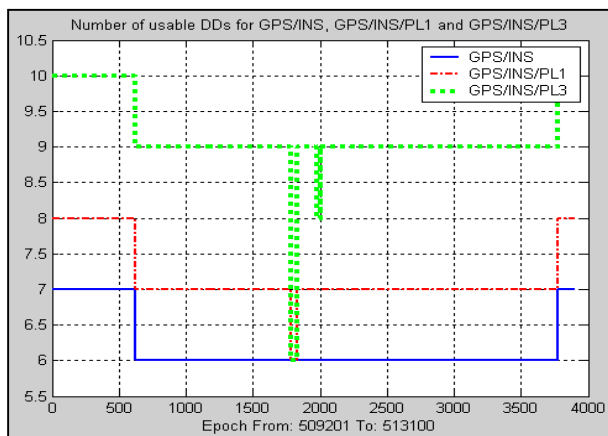


Figure 2. Number of double differences for GPS and PLs.

| RMS Diff. | Mean  | Standard deviation | Max    | Min   | Unit   |
|-----------|-------|--------------------|--------|-------|--------|
| N         | 1.98  | 3.22               | 29.40  | 0.10  | mm     |
| E         | 2.62  | 7.81               | 49.81  | -2.64 | mm     |
| Ht        | 12.07 | 28.50              | 198.45 | 0.33  | mm     |
| Vn        | 0.08  | 0.04               | 0.30   | 0.03  | mm/s   |
| Ve        | 0.05  | 0.09               | 0.52   | -0.10 | mm/s   |
| Vd        | 0.32  | 0.50               | 2.91   | 0.02  | mm/s   |
| Heading   | 1.09  | 2.06               | 9.59   | -0.16 | arcsec |
| Pitch     | 0.08  | 0.11               | 9.59   | -0.16 | arcsec |
| Roll      | 0.03  | 0.03               | 9.59   | -0.16 | arcsec |

Table 3. RMS Difference in position, velocity and orientation between GPS/INS solutions using four highest satellites and the same satellites supported by three PLs

An example presented here clearly indicates that PL technology can provide a viable augmentation to GPS/INS. It is not expected, however, that it will soon become a standard technique for GPS augmentation in precise positioning; however, specialized applications are expected to be developed, based on portable array of PLs that can be deployed at the mapping area in a campaign mode. More research is also needed to resolve the problems of possible biases in PL signal and PL-based multipath.

### 3. MULTI-SENSOR CALIBRATION

With a significant progress in the accuracy and operational flexibility of imaging sensors used commonly in mapping and remote sensing, the aspect of sensor/data fusion aimed at providing optimal and rich in content geospatial information, has become an important research topic in the past few years. Consequently, more and more systems developed recently are based on multiple image sensor suites, creating common framework for better, faster and cheaper generation of terrain and surface models, together with better object recognition. Smart data fusion for terrain and surface generation, based on entirely digital data sources, enables a high level of automation of terrain and surface updating processes, as well as rapid change detection. Some examples of multi-sensor data fusion for thematic mapping and urban modelling are presented in the

sequel. However, for multi-sensor systems to function properly, the issue of reliable georeferencing (georegistration) and calibration must be properly addressed. Individual sensor calibration, as well as sensor inter-calibration are crucial for an accurate and reliable operations of any multi-sensor mapping system, especially when the highest accuracy is required. The multi-sensor calibration includes GPS/INS lever arms (usually obtained from precision surveying, but can also be corrected during the positioning adjustment), and boresight calibration between the navigation sensor and the imaging frames. The issue of multi-sensor calibration has been addressed in the literature; see for example (Grejner-Brzezinska et al, 1999; Grejner-Brzezinska, 2001a and b; Moustafa, 2001; Toth and Csanyi, 2001; Toth et al., 2002).

### 3.1 Boresight Calibration Between GPS/INS and Imaging Sensors

Boresight, defining the transformation between the georeferencing sensors (GPS/INS) and the imaging sensors, is a crucial component of the multi-sensor systems calibration, especially for the highest accuracy mapping applications. The critical components are the rotational offsets, since any angular inaccuracy, unlike a linear offset, is amplified by the object distance and has a significant impact on the photogrammetric data production, especially in airborne scenario. The boresight transformation is most commonly resolved by comparing the GPS/INS positioning/orientation results with an independent AT solution (see an example below), or as a part of a bundle adjustment with constraints (see for example El-Sheimy et al. 1995). Thus, the quality of the boresight estimation is limited by the quality of the AT adjustment and the quality of the direct orientation components that are used in the boresight estimation process. Consequently, the availability of a high quality test range with very well signalised points for AT, which should be used for the calibration process becomes an important issue.

An example solution of boresight transformation estimation, including the quality assessment for a land-based system is presented in Tables 4 and 5. The boresight estimates presented in Table 4 were obtained as angular and linear differences between the AT and GPS/INS solutions. A ground-based test range, with coordinates surveyed by differential GPS (accuracy of 1-2 cm), was used for AT. The camera used was Pulnix TMC-6700, based on 644 by 482 CCD, with the effective pixel size on the ground of 4.1 mm at nadir, at the object distance of about 3 m. These transformation parameters were used in combination with DPO parameters, to check an independent set of control points, as shown in Table 5. Even though the boresight angle accuracy does not seem very high (due primarily to a low resolving power of the camera), the ground truth provides very good results, as the object distance in that MMS is rather short, as the imaging sensor is a down looking camera.

| Offset<br>In IMU body<br>frame [m] |        | RMS<br>[m] | Misalignment<br>Angles [deg] |         | RMS<br>[deg] |
|------------------------------------|--------|------------|------------------------------|---------|--------------|
| <b>x</b>                           | -1.007 | 0.0044     | $\omega$                     | 2.2817  | 0.4054       |
| <b>y</b>                           | 0.046  | 0.0280     | $\phi$                       | 11.2003 | 0.1274       |
| <b>z</b>                           | 0.450  | 0.0090     | $\kappa$                     | 87.7725 | 0.0388       |

Table 4. Boresight transformation estimation.

| Model<br>Check<br>points | Coordinate Difference |        |        |
|--------------------------|-----------------------|--------|--------|
|                          | N                     | E      | h      |
| <b>461</b>               |                       |        |        |
| <b>12 1</b>              | -0.007                | -0.001 | -0.007 |
| <b>12 2</b>              | 0.024                 | -0.017 | -0.061 |
| <b>3</b>                 | 0.012                 | -0.001 | -0.067 |
| <b>4</b>                 | 0.006                 | 0.001  | -0.049 |
| <b>462</b>               |                       |        |        |
| <b>0</b>                 | 0.014                 | 0.029  | -0.121 |
| <b>12</b>                | 0.024                 | 0.009  | -0.040 |
| <b>4</b>                 | 0.003                 | -0.020 | -0.085 |
| <b>45</b>                |                       |        |        |
| <b>12</b>                | -0.014                | 0.028  | -0.044 |
| <b>4</b>                 | -0.008                | -0.010 | -0.028 |
| <b>3</b>                 | 0.015                 | -0.015 | -0.094 |
| <b>0</b>                 | 0.010                 | -0.034 | -0.043 |

Table 5. Difference between the surveyed checkpoints and their coordinates derived from directly oriented imagery.

Another approach to boresight estimation is to perform high-accuracy measurement of boresight linear offsets, as INS and the imaging sensor are usually rigidly connected, and estimate the boresight angles as a difference between GPS/INS and AT solutions. An example of the achievable accuracy indicates that linear offsets can be measured with mm-level accuracy, and the final estimation of angular components is limited by the accuracy of GPS/INS and AT. With a high-resolution aerial camera (such as RC30 and RMK-TOP or LMK 2000) and quality AT based on sufficiently strong geometry, good quality imagery with precise measurements, and high-accuracy GPS/INS results (1-2 cm in horizontal, 2-3 cm in vertical), the accuracy of boresight angles of 20-30 arcsec is feasible. For example, the errors in boresight angles of 20-60 arcsec and 2 cm in offsets, translate to about 2-5 cm error (per coordinate) on the ground for 300 m object distance. The analysis of the impact of the boresight angle errors on the ground coordinates are presented in more detail in (Grejner-Brzezinska, 2001b).

In a recent airborne test conducted by ODOT and OSU with the Applanix POS/AV 510-DG and LMK 2000 camera, the linear offsets were surveyed with mm-level accuracy, and the boresight angles were estimated as differences between high accuracy GPS/INS and AT solutions. The resulting accuracy on the ground, for ~350 m object distance reached 2-5 cm in horizontal, and 3-8 cm in vertical directions.

LIDAR boresight calibration is a crucial component of any mapping system based on this sensor, primarily due to the fact that LIDAR systems are rather complex, and include at least three main sensors, GPS and INS, and the laser-scanning device (Figure 3 illustrates a common sensor configuration of airborne LIDAR systems). The laser system offers few-cm accuracy in measuring the distances from the sensor to the ground surface. If the laser beam orientation and the position of the laser scanner are known, the coordinates of the ground reflection point can be calculated based on the travel distance (time) of the laser pulse. Since LIDAR relies entirely on direct orientation, any GPS/INS positioning errors or misalignment between the laser and the navigation systems will translate to an error in the surface point coordinates. In general, the lack of feedback in the data flow in LIDAR systems makes the whole system more vulnerable to systematic errors and that may seriously affect the quality of the LIDAR data (Toth et al, 2002).

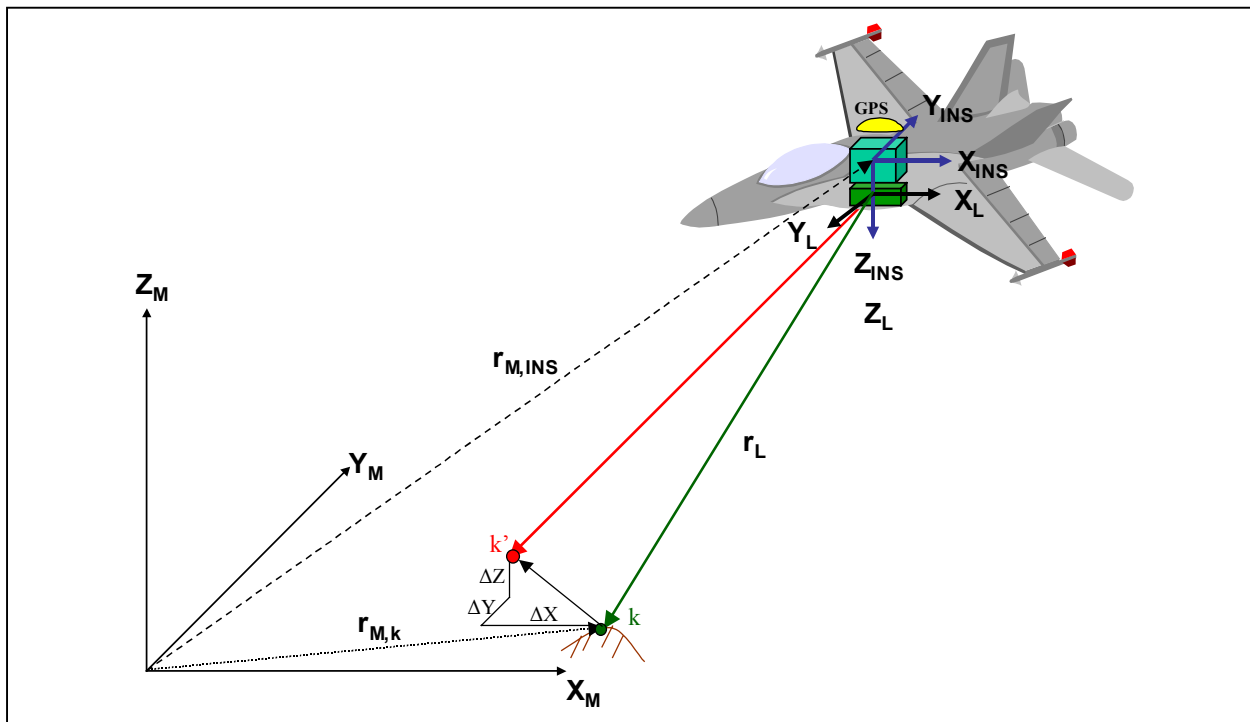


Figure 3. LIDAR system sensor configuration:  $XYZ_L$  is the LIDAR reference frame,  $XYZ_{INS}$  is the INS body frame and  $XYZ_M$  is the local mapping frame;  $\Delta X, \Delta Y, \Delta Z$  denote errors on the ground due to the boresight misalignment.

Boresight misalignment can be determined provided that sufficient ground control is available. An alternative solution, proposed by (Toth et al., 2002; Toth, 2002), independent from ground control, is based on overlapping LIDAR strips flown in different directions, collected over an unknown surface (ground truth information can also be incorporated, if available). In addition, precise navigation data (GPS/INS) are required. The approximate values of the three rotation angles between the INS and the laser frames are known from the mechanical alignment. The remaining difference (misalignment) between the nominal and actual angles must be determined. In this method, the horizontal and vertical discrepancies between the overlapping LIDAR strips are used to determine the unknown misalignment angles. Generally, more reliable results can be obtained if a number of strips are used. Also, the surface differences must be observed in specifically select areas, where the differences are mostly pronounced. For example, surface patches closer to the borders of the overlapping area, similar to the Gruber point distribution in stereo photogrammetry, are very suitable. It should be pointed out that comparing different surfaces, formed by randomly scattered points is a non-trivial task, and the effectiveness of this process depends a lot on the point density of the LIDAR points and on the overall terrain characteristics of the overlapping area. Therefore, the random point distribution is interpolated into a regular grid, allowing for the surface discrepancies to be found relatively easily by surface matching of the selected regions or profile matching of man-made objects, etc.

The next step, after the surface discrepancies have been determined at certain regions of the overlapping area, is to perform a least squares adjustment, with the surface differences as observations, and parameterised with the unknown misalignment angles. Based on the observed differences (in 3D), the misalignment angles are iteratively adjusted to reduce the

surface discrepancies in object space. The sequence of operations implemented is as follows: segmentation of the overlapping area (smoothly rolling terrain is the best selection), interpolation into a regular grid, matching the segments (finding the 3D differences between the selected and interpolated small segments of the overlapping area; can be formed between any pairs of LIDAR data strips), least squares adjustment. The details of the procedure can be found in (Toth et al., 2002).

#### 4. APPLICATIONS: MAPPING AND GIS

##### 4.1 Mapping Applications

Mobile mapping technology has been employed in a number of important real-life applications. Airborne mobile mapping systems have mainly been used for the same purposes as traditional aerial mapping technology. However, because they use digital imaging sensors and avoid or greatly reduce ground control requirements, MMS provide much higher efficiency than traditional aerial mapping. Land-based MMS, on the other hand, have mainly been used in highway and facility mapping applications in which traditional terrestrial mapping technology is either impossible or very inefficient to apply. Over the past decade, the uses of both airborne and land-based mobile mapping technology have been notably expanding in many new directions.

There are several advantages to using mobile mapping technology in highway applications. Because it employs dynamic data acquisition, mobile mapping technology can be directly used in highway-related applications such as traffic sign inventory, monitoring of speed limits and parking violations, and generation of road network databases. When laser technology is jointly applied, road surface condition inspection can also be achieved. As long as traffic velocity is less than

approximately 70 km per hour, data acquisition can be performed without disturbing traffic flow. In addition, a single collection of data can be used to obtain diverse information for multiple purposes. Moreover, because data can be both collected and processed in a short time period, frequent repetition of road surveys and updating of databases are both possible and affordable.

Automatic and semi-automatic methods have been researched for the extraction of road and highway features such as road centrelines as well as road signs, traffic lights and road curb lines. Once extracted, these objects can be automatically organized into spatial databases. In order to extract a road centreline, an image sequence of the road is needed where each image pair supplies one segment of the entire centreline. Using land based MMS imagery, successive road segments are measured and then combined to produce the entire road centreline. From each image sequence, centreline features are automatically enhanced and extracted. Corresponding 3D centreline segments are then generated in object space (He and Novak, 1992). A different approach defines a 3D centreline in object space as a physical Snake Model (Tao et al., 1996; 1998). The Snake Model is optimized to adjust the centreline shape using image features of the centreline as internal constraints and using geometric conditions derived from other sensors of the system (GPS and INS) as external constraints. Habib et al. (1999) have presented an algorithm for automatic extraction of road signs from color imagery using feature detection, hypothesis generation and verification techniques. Tu and Li (2002) have proposed a framework for automatic recognition of spatial features from mobile mapping imagery based on the view-dependent method along with hypothesis test techniques and they have demonstrated its application in the recognition of traffic lights. Road curb lines (as opposed to painted centrelines) are projected onto the images based on their geometric shapes and material types. Consequently, curb lines can be more difficult to automatically extract and identify. Currently, curb line databases are built using semi-automatic or manual approaches.

Another MMS, recently developed at The Ohio State University, is focused on real-time centerline mapping using single down-looking digital camera (Pulnix TMC-6700, based on 644 by 482 CCD, with an image acquisition rate of up to 30 Hz), oriented by high-accuracy tightly coupled GPS/INS system. The main goal of the on-the-fly image processing is to determine the centerline image coordinates in real time, so that only the automatically extracted polyline, representing the center/edge lines would be stored, without a need to store the entire image sequence. In particular, the linear features can be extracted from the imagery on-the-fly, using real-time navigation information used to form stereo-pairs. Thus, for the real-time part of the image processing only relative orientation (RO) is important, while the final processing can be done in post-mission mode, when more precise navigation data become available. Typically, even in post processing the feature extraction task requires substantial user interaction. Since our system uses a down-looking camera, with an image sensor plane almost parallel to the road surface, the image scale changes are negligible, thus an almost constant scale along the vehicle trajectory can be maintained. Moreover, the object contents of the images are rather simple and predictable, such as the line marks, surface texture variations, cracks, potholes, skid marks, etc. Consequently, extracting features from a predefined set of objects, assuming almost constant image scale, represents a less challenging scenario, as compared to the generic MMS

paradigm, where the scale variations (and the richness of features) pose serious difficulty for any automated feature extraction task.

Stereovision is realized by the platform motion, which, in turn, emphasizes the need for high-precision sensor orientation provided by direct georeferencing. In essence, the real-time image processing is technically feasible due to a simple sensor geometry (see Figure 4) and limited complexity of the imagery collected (images of the pavement with about 50% overlap, where only linear features are of interest). Feature points are extracted around the centerline area, and are subsequently used for image matching. Note that the availability of the relative orientation between the two consecutive images considerably decreases the search time for conjugate entities in the image pair, since the usually 2D search space can be theoretically reduced to one dimension, along the epipolar lines. However, errors in orientation data introduce some uncertainty in the location of the epipolar line, stretching it to an epipolar band, whose width depends on the accuracy of EO parameters.

An example of image processing sequence is presented in Figure 5. In our standard image processing the following steps are included: RGB to S transformation, median filter and binary conversion (thresholding), centreline boundary point extraction, all based on a single image, and subsequently, feature matching, affine transformation and centreline strip formation, performed in stereovision (Toth and Grejner-Brzezinska, 2001).



Figure 4. Sensor assembly for real-time centreline mapping.

Location and measurement of cracks and crevices in road surfaces are a major goal of road inspections. If an MMS is equipped with laser sensors, differences between the sensor readings and the road surface are available as relative depth measurements. If control data from the GPS and INS are also available, this relative data can be integrated into the global reference system and used to generate a digital road surface model that includes detailed variances in the road surface. This surface model can then be used to identify the location, size, and shape of crevices in the road surface.

Another major use of mobile mapping technology lies in the field of facility mapping. For example, high-voltage power transmission lines can be photographed by a mobile mapping system and their position then measured using the resulting image sequences. A number of important parameters can be calculated from the resulting data including the position of poles and towers. In addition, the position of insulators on each line that supports the suspending transmission line segments

can be located as well as the lowest point of each of the suspending line segments. To this purpose, Li et al. (1999) have presented a method based on Hopfield neural networks for utility object detection and location, particularly for streetlights, from mobile mapping image sequences.

Mobile and real-time mapping technologies are being applied to a number of new applications in addition to their primary use in highway and facility mapping (Li et al., 2001). These include (but are not limited to) automatic bald digital terrain model reconstruction using airborne SAR, Mars landing site mapping and rover localization, integration of data from terrestrial mobile mapping systems and aerial imagery for change detection purposes, integration of photogrammetric data from mobile ship-borne and airborne systems for support of conservation processes and environmental analysis, automatic building extraction from airborne laser systems, and integration of mobile phone location services into intelligent GPS vehicle navigation systems.

**4.2 Mobile GIS**

Mobile GIS is one of the latest useful services that have come out of the inexpensive access capabilities provided by the new wireless Internet and mobile mapping capability. Its development has been stimulated by increasing demand for up-to-date geospatial information, along with technological improvements in hardware size, performance, power consumption and network bandwidth (Maguire, 2001).

Mobile GIS applications can deliver mapping output in a number of different formats including text, image, voice, and video in field. Information can be requested from Internet servers using the wireless application protocol-based Wireless Markup Language (WML). Resulting maps can be displayed in the form of an embedded map (Maguire, 2001). Along with many others, GIS software market leaders AutoDesk, ESRI and Intergraph are currently developing software and system architecture for mobile GIS applications.

Compared with the traditional GIS applications, mobile mapping/mobile GIS technology has two unique components: 1) portable mobile devices, such as wireless telephones and PDAs, serving as client terminals and 2) a wireless network. Wireless telephones can access data in three different ways: Wireless Application Protocols (WAP), General Packet Radio Service (GPRS), and I-Mode. Using special wireless services (such as GoAmerica) or a wireless modem, PDA users can access content through the Internet with WindowsCE-based Internet Explorer or other WAP-capable browsers. Current applications of mobile GIS include field mapping, routing, tracking, data collection, and public safety. Two popular uses of the technology are routing and facility search (Srinivas et al., 2001).

Restrictions of the current mobile GIS technology include a limited number of service providers, who offer wireless data transfer services and limited wireless bandwidth. The current transfer speed through CDMA (Code Division Multiple Access) WAP wireless telephones is about 9.6 kbps. The speed of GPRS WAP telephones is about 53.6 kbps. These transfer speeds would be unacceptable for use in transferring large spatial data sets, such as those found with remote sensing data. As the technology improves, mobile GIS will become much more accepted, especially when wireless data transfer speeds are greatly increased with the introduction of the third-generation (3G) communication system, expected in the next few years.

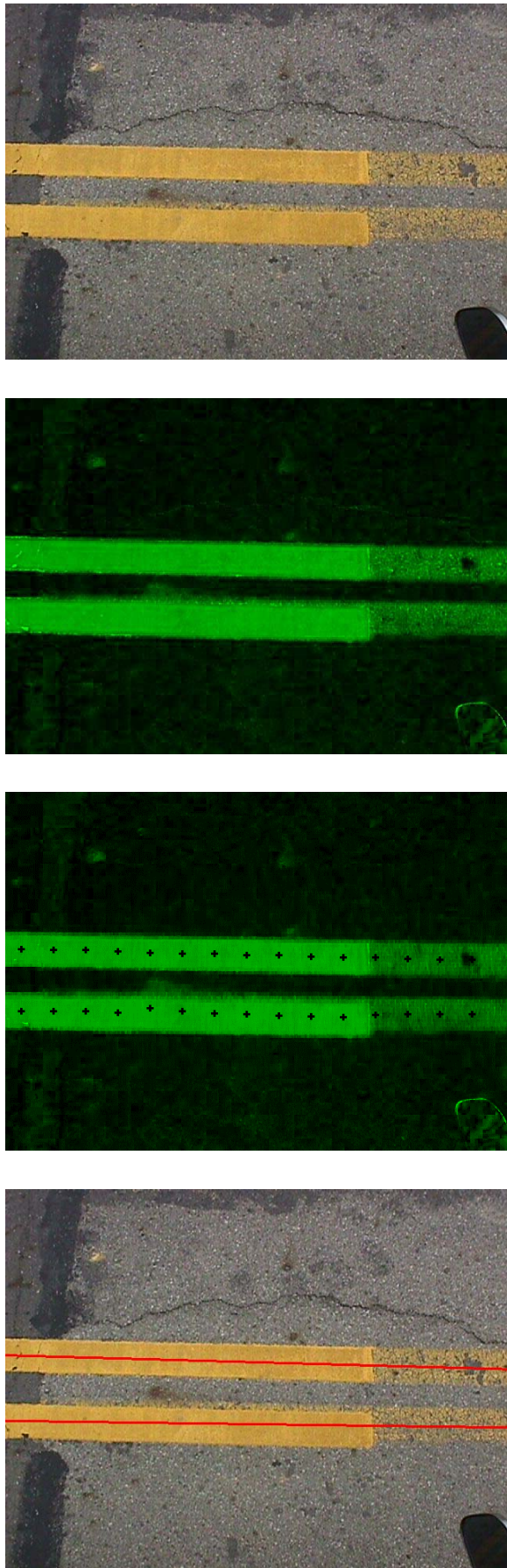


Figure 5. Image sequence processing in real-time.



Another emerging discipline, with its roots in mobile mapping technology, is telegeoinformatics, which integrates the theory and applications of geospatial informatics (geoinformatics), telecommunication, and mobile computing technologies. Geoinformatics, as a foundation component of telegeoinformatics, is based on GIS, which utilizes remote sensing and geolocation techniques such as GPS/INS, to gather attribute and geospatial information. Telegeoinformatics directly exploits geoinformatics, i.e., GIS, GPS, satellite imagery and aerial photography in a mobile computing environment, where the mobile computers are linked through a wireless communication network. The next milestone for telegeoinformatics is the development of Location-Based Computing (LBC) and Location-Based Services (LBSs), expected in the next few years ([http://www.isr.umd.edu/~caseymj/documents/presentations/2001\\_RRD\\_Poster.pdf](http://www.isr.umd.edu/~caseymj/documents/presentations/2001_RRD_Poster.pdf); <http://www.dvo.ru/bbc/pdpta/vol4/p368.pdf>)

#### 4.3 Thematic mapping by multi-sensor systems

In addition to establishing the platform orientation, the image-based extraction of topographic objects like buildings, streets, trees, or other land use classes, is an important goal of photogrammetric processing. Geometric and semantic information for the reconstruction of the depicted objects can be extracted easily by a human operator. However, a full automation of this process has so far remained an unsolved task. Up to now, an automatic image interpretation is mainly feasible for applications restricted to well defined environments and/or simple objects that can be frequently found in, for example, indoor industrial environments. Thus, in order to enable automatic interpretation for very complex outdoor scenes, as desired for topographic mapping, additional sources of information must be provided from multi-sensor systems. In addition to standard (monochromatic) images, these systems may provide, for example, LIDAR data as well as multi-spectral imagery.

The potential of multi-sensor systems and integrated data processing to improve the degree of automation and reliability of photogrammetric data collection and interpretation, is demonstrated here by the two following examples. The first example illustrates how combination of the spectral data from images and point data from LIDAR can be used for thematic mapping in complex built-up areas. The second example applies the same types of information as well as already existing 2D GIS data for the automatic collection of 3D city models.

##### 4.3.1 Classification of Urban Areas

Spectral information has been widely used as a data source for thematic mapping applications, which are based on traditional classification techniques. In the past, the classification of remotely sensed data has been mainly limited to space-borne systems with a ground sampling distance of several meters. This situation has changed dramatically due to the availability of modern high-resolution spaceborne sensors, and even more importantly due to the development of commercially available digital airborne cameras. These systems provide image data with a radiometric resolution and quality comparable to the satellite missions, with a geometric resolution down to 10 cm. Since traditional remote sensing techniques can now be applied to high-resolution digital aerial imagery, applications like large-scale mapping and the extraction of man-made structures in complex urban scenes should become possible. Nevertheless, if the available information is restricted to multispectral data only,

the classification of urban land use does not lead to precise and consistent interpretation, since higher spatial resolution mostly widens the variance of classes, leading to some misinterpretations. Especially during the thematic mapping of man-made structures, the same colours in the same data set might indicate different objects, thus the accuracy and reliability of the results is limited.

A common goal during the data acquisition in built-up areas is the detection of objects like streets and buildings. However, this can be difficult if only spectral information is used, since for some areas roofs and streets are built of very similar materials. This complicates or even prevents the discrimination of these objects due to their similar reflectance properties. The same problem can arise, if trees and grass-covered areas have to be differentiated. In order to demonstrate the insufficiency of a standard classification restricted to the analysis of a multispectral information only, a maximum likelihood classification was applied to a section of a Color-Infrared (CIR) aerial image. The result of the separation into the required object classes is depicted in Figure 6.

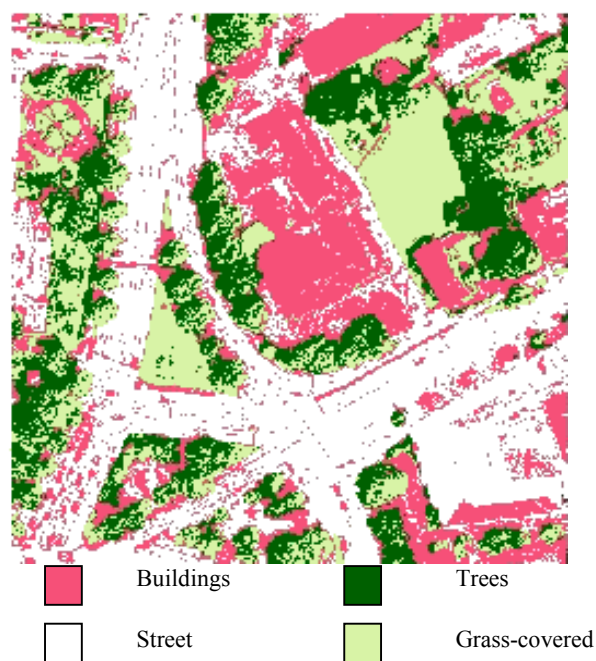


Figure 6. Classification based on CIR imagery

This situation improves significantly if a Digital Surface Model (DSM), resulting from airborne laser scanning is combined with the multispectral aerial image. In order to separate objects like trees and buildings from their surroundings, an information on the local height above the terrain can be very valuable, since these types of objects are higher than their surroundings, whereas other objects of interest like streets and grass-covered areas are at the terrain level. To make the required geometric information accessible the so-called normalised DSM, i.e. the difference between the Digital Surface Model (DSM), which is provided by airborne laser scanning DSM, and the Digital Terrain Model (DTM) has to be calculated. The required DTM can be derived from the DSM based on mathematical grey scale morphology, which eliminates all local maxima in height of a predefined size. The normalised DSM then provides a representation of all objects above the terrain, located approximately on a plane.

Multi-spectral data enables a good separation between vegetation and non-vegetation areas. The vegetation areas can then be separated into tree regions (high values of the normalized DSM) and other vegetation like grass-covered areas (low values of the normalized DSM). Accordingly, the non-vegetation areas can be differentiated into buildings (high areas) and non-building regions like streets (low areas). In order to integrate the geometric information as provided by the normalised DSM and the complementary multispectral information, a standard classification algorithm can be applied. For this purpose the information on the local height above the terrain is integrated as an additional channel in combination with the spectral channels as provided from the CIR aerial image.

Figure 7 demonstrates the improved extraction of the required object classes. Due to the hardware limitations, LIDAR data from this project were combined with multi-spectral information provided from the scanned CIR aerial images (Haala and Brenner, 1999); the classification of urban environments, based on data from the a digital airborne camera, has been demonstrated by (Hoffman et al., 2000).

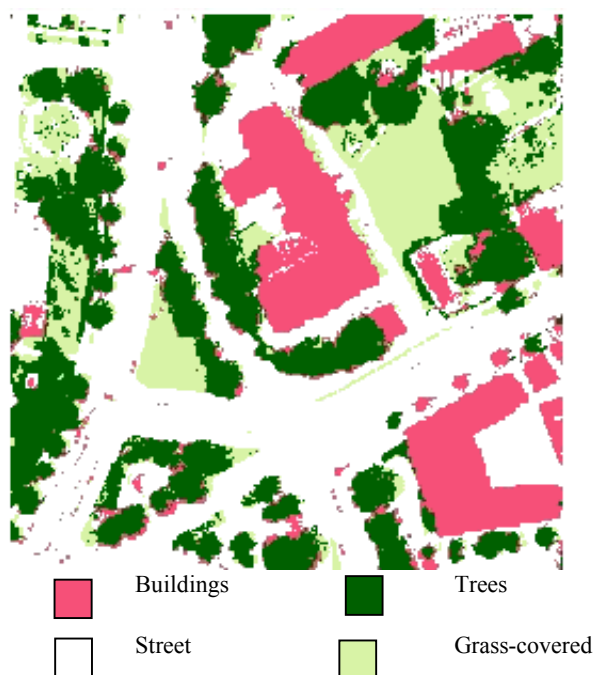


Figure 7. Classification based on CIR imagery and laser data

#### 4.3.2 Automatic Collection 3D City Models

Three-dimensional city models are usually comprised of a description of the terrain, streets, buildings and vegetation in build-up areas. Since there are numerous possible applications for this type of data, including architecture and town planning, virtual trip planning and tourist information systems, car and personal navigation systems and simulations for microclimate, air pollution, and propagation of noise or electromagnetic waves, a lot of effort has been spent on automatic and semi-automatic collection of 3D city models. A good overview can be found in (Baltsavis et al., 2001). In general, automatic 3D building reconstruction from aerial images has shown promising results, however the reliable extraction of buildings in densely build-up areas has not been demonstrated yet. On the other hand DSMs as acquired by laser scanning represent the

geometry of the surface directly, thus they have advantages related to automated interpretation. A fully automatic 3D building reconstruction can be achieved if 2D ground plans of the buildings are used in addition to LIDAR data (Brenner and Haala, 2001). These ground plans are frequently available from existing GIS, alternatively they can be obtained by manual extraction from maps or plans. In each case, the ground plans represent a certain amount of interpretation by the operator, which helps for the following automatic 3D reconstruction.

Within this approach the ground plan is used to infer on how the building can be subdivided into primitives. The decomposition of complex buildings is based on the assumption that a high percentage of buildings can be modelled using a small number of building primitives like flat boxes, boxes with saddleback and hipped roofs, and other geometric primitives like cylinders and cones. Even if one considers only primitives based on rectangular ground shapes as it is realised in the algorithm, still the majority of buildings can be modelled. Each 2D primitive, resulting from ground plan decomposition, is the footprint of a corresponding 3D primitive. The location, orientation, and size of the 2D primitive apply as well to the 3D primitive. What remain to be determined, are the parameters of the roof, namely roof type (flat, gable or hip), height of the building and the roof slope. A least squares estimation computes the best fit of the models to the given DSM. When several models are suitable, the one with the smallest residual is selected. After this step, the individually reconstructed primitives are overlapping 3D solids, which are merged to a boundary representation by a CAD kernel.

Recently, this approach has been used in a large number of projects. Figure 8 gives an example of a reconstruction of the city of Lindau, Germany. Even though the geometry of the reconstructed buildings presented here is entirely based on the automatic interpretation of LIDAR and 2D GIS data, it must to be noted that for many applications, additional information is necessary. Realistic visualisation can, for example, be obtained only when the texture of the ground, roofs and façades is present. In order to simultaneously provide the required image data, the LIDAR sensor was collocated with a digital camera. If required, these images can also be used for semi-automatic refinement of the 3D building reconstruction. Compared to the LIDAR data, the images provide a higher geometric resolution, which helps the visual interpretation.



Figure 8. 3D city model reconstructed from LIDAR data.

## 5. SUMMARY

In this paper, an overview of the mobile mapping technology and its land-based and airborne applications was provided. The notion of direct georeferencing and its basic operational aspects was also discussed. The importances of the multi-sensor system calibration, with some examples of the currently achievable accuracy were presented.

Some examples, of the state-of-the-art applications presented here, illustrate well the ability of multi-sensor systems as important mapping/GIS tools, enabling the much-desired automation of photogrammetric data collection and interpretation. The aspect of real-time mobile mapping/mobile computing, based on GPS/INS, automatic image processing and telecommunication networks were indicated as the newest trends in MMS technology development. Although some tasks, related to calibration and image data processing can be done automatically, in many cases a human operator is needed. Thus, more research in the area of automatic interpretation and image data fusion are expected in the nearest future. Still, it is fair to expect that these topics, as extremely challenging, may not be resolved in the next decade or two. On the other, the advancements in mobile GIS and telegeoinformatics indicate that Location-Based Computing and Location-Based Services may shortly become a widespread reality.

In summary, a mobile mapping technology initiated over a decade ago has substantially evolved to a level of sophistication and automation not viable at its outset. Proliferation of the navigation and image sensor technology, state-of-the-art computing power and easy access to relatively inexpensive telecommunication services totally redefined the early paradigm of mobile mapping. Its current level of advancements and still expected improvements in sensor and data processing technologies, as well as ever-extending market can only indicate that, indeed, mobile mapping is a technology of the future.

## REFERENCES

- Abdullah, Q., 1997. Evaluation of GPS-Inertial Navigation System for Airborne Photogrammetry, presented at 1997 ACSM/ASPRS Annual Convention and Exposition, April 7-10, Seattle, WA.
- Axelsson, P., 1999 Processing of Laser Scanner data – Algorithms and Applications, *ISPRS Journal of Photogrammetry and Remote Sensing*, No. 54, pp.138-147.
- Baltsavias, E., A. Grün and L. van Gool (eds.) 2001. Automatic Extraction of Man-Made Objects from Aerial and Space Images (III) A.A, Balkema Publishers, 415 pages.
- Baltsavias, E.P. 1999. Airborne laser scanning: basic relations and formulas. *ISPRS Journal of Photogrammetry & Remote Sensing*, 54, pp. 199-214.
- Barnes, J., Wang, J., Rizos, C., Ttsuji, T. 2002. *The Performance of a Pseudolite-Based Positioning System for Deformation Monitoring*, 2<sup>nd</sup> Symposium on Geodesy for Geotechnical and Structural Engineering, Berlin, Germany, May 21-24, pp. 326-337.
- Bossler, J. D., Goad, C., Johnson, P., and Novak, K., 1991. GPS and GIS Map the Nation's Highway, *GeoInfo System Magazine*, March, pp. 26-37.
- Bossler, J. D., and Toth, C., 1995. Accuracies Obtained by the GPSVan™, *Proc. GIS/LIS'95*, Vol. 1., pp. 70-77.
- Brenner, C. & Haala, N. 2001. Automated Reconstruction of 3D City Models. In: *Abdelguerfi M. (ed.), 3D Synthetic Environment Reconstruction*, Kluwer Academic Publishers, pp. 75-101.
- Da, R., 1997. Investigation of Low-Cost and High-Accuracy GPS/IMU System, *Proc. ION National Technical Meeting, Santa Monica*, pp. 955-963.
- El-Sheimy, N., Schwarz, K. P., Gravel, M. 1995. Mobile 3-D Positioning Using GPS/INS/Video Cameras, *Proc. Mobile Mapping Symposium, OSU Center for Mapping*, pp. 236-249.
- Ford T., Neumann J., Toso N., Petersen W. Anderson C and Fenton P. HAPPI – a High Accuracy Pseudolite/GPS Positioning Integration. *Proceedings ION GPS*, 1996: 1719-1728, Kansas City, Missouri, September 17-20.
- Grejner-Brzezinska D. A., Yi Y. and Wang J. 2002. Design and Navigation Performance Analysis of an Experimental GPS/INS/PL System, *Proc. 2<sup>nd</sup> Symposium on Geodesy for Geotechnical and Structural Engineering*, Berlin, Germany, May 21-24, pp. 452-461.
- Grejner-Brzezinska D. 2001a. Mobile Mapping Technology: Ten Years Later, Part I, *Surveying and Land Information Systems*, Vol. 61, No.2, pp. 79-94.
- Grejner-Brzezinska D. 2001b. Mobile Mapping Technology: Ten Years Later, Part II, *Surveying and Land Information Systems*, Vol. 61, No.3, pp. 83-100.
- Grejner-Brzezinska D. A., Toth C. K. and Edward Oshel 1999. Direct Platform Orientation in Aerial and Land-Based Mapping Practice, Real Time Mapping Technologies, ISPRS Working Group II/1, Bangkok, Thailand, April 21-23, 1999, pp. 2-4-1—2-4-7.
- Grejner-Brzezinska D. A., Phuyal B. P., 1998. Positioning Accuracy of the Airborne Integrated Mapping System, *Proc. ION Technical Meeting*, Long Beach, CA, pp. 713-721
- Grejner-Brzezinska, D. A., 1997. Airborne Integrated Mapping System: Positioning Component, *Proc. 53rd ION Annual Meeting*, Albuquerque, NM, pp. 225-235.
- Haala, N. and Brenner, C. 1999. Extraction of buildings and trees in urban environments. *ISPRS Journal of Photogrammetry and Remote Sensing* 54[2-3], pp:130-137
- Habib, A.F., R. Uebbing, and K. Novak, 1999. Automatic Extraction of Road Signs from Terrestrial Color Imagery. *Photogrammetric Engineering and Remote Sensing*, 65(5): 597-601.
- He, G.P. and Novak, K., 1992. Automatic Analysis of Highway Features from Digital Stereo-Images, *International Archives of Photogrammetry and Remote Sensing*, Vol. XXIX, part B3, ISPRS Comm. III, pp. 119-124.
- He, G.P., Novak, K., and Tang, W. 1994. The Accuracy of Features Positioned with the GPSVan, *Symp. ISPRS Comm. II Symposium*, Vol. 30, Part 2, pp. 480-486.
- He, G. Orvets, G. and Hammersley, R., 1996. Capturing Urban Infrastructure Data Using Mobile Mapping System, *Proc. 52<sup>nd</sup> ION Annual Meeting*, pp. 667-674.

- Hoffmann, A., van der Vegt, J. & Lehmann, F. 2000, Towards Automated Map Updating: Is it feasible with new digital data-acquisition and processing techniques in IAPRS Vol. 33 Part B2, pp. 295-302.
- Lee, H-K., Wang, J. and Rizos, C. 2002. Kinematic Positioning with an Integrated GPS/Pseudolite/INS, *2<sup>nd</sup> Symposium on Geodesy for Geotechnical and Structural Engineering*, Berlin, Germany, May 21-24, pp. 314-325.
- LeMaster E. and S. Rock 1999. Mars exploration using self-calibrating pseudolite arrays. *Proceedings, ION GPS*, Nashville, Tennessee, September 14-17. pp. 1549-1558.
- Li, R., W. Wang, and H.-Z. Tseng, 1999. Detection and Location of Objects from Mobile Image Sequences by Hopfield Neural Networks. *Photogrammetric Engineering and Remote Sensing*, 65(10), pp.1199-1205.
- Li, R., N. Haala, and K. Di, 2001. Annual Report of ISPRS Working Group II/1. Available at <http://shoreline.eng.ohio-state.edu/wg2-1/wii-1-rep-00-01.html>.
- Lithopoulos, E., Reid, B., Scherzinger, B., 1996. The Position and Orientation System (POS) for Survey Applications, *International Archives of Photogrammetry and Remote Sensing, ISPRS Comm. III*, Vol. XXXI, part B3, pp. 467-471.
- Maguire, D. 2001. Mobile Geographic Services. Map India 2001, <http://www.gisdevelopment.net/technology/mobilemapping/techmp003.htm>.
- Meng, X., Roberts, G. W., Doodson, A. H., Cosser, E., Noakes, C. 2002. Simulation of the Effects of Introducing Pseudolite Data into Bridge Deflection Monitoring Data, *Proc. 2<sup>nd</sup> Symposium on Geodesy for Geotechnical and Structural Engineering*, Berlin, Germany, May 21-24, pp. 372-381.
- Mostafa, M. 2001. Calibration in Multi-Sensor Environment, *Proc. ION GPS*, pp. 2693-2699.
- Srinivas, U., S. M. C. Chagla, V. N. Sharma, 2001. Mobile Mapping: Challenges and Limitations. Map India 2001, <http://www.gisdevelopment.net/technology/mobilemapping/techmp004.htm>.
- Schwarz, K. P., Wei, M., 1994: Aided Versus Embedded A Comparison of Two Approaches to GPS/INS Integration, *Proceedings of IEEE Position Location and Navigation Symposium*, Las Vegas, NE, pp. 314-321.
- Schwarz, K. P., Chapman, M., Cannon, M. E., and Gong, P., 1993: An Integrated INS/GPS Approach to the Georeferencing of Remotely Sensed Data, *PE&RS*, Vol. 59, No. 11, pp. 1667-1674.
- Tao, C., R. Li, and M.A. Chapman, 1996. Model Driven Extraction of Road Line Features Using Stereo-Motion Constraints from a Mobile Mapping System. *ACSM/ASPRS 96*, pp. 135-144.
- Tao, C., R. Li, and M.A. Chapman, 1998. Automatic Reconstruction of Road Centerlines from Mobile Mapping Image Sequences. *Photogrammetric Engineering and Remote Sensing*, 64(7), pp. 709-716.
- Toth, C. 2002. Calibrating Airborne LIDAR Systems, *in this volume*.
- Toth C., Csanyi N. and Grejner-Brzezinska D. 2002. Automating The Calibration Of Airborne Multisensor Imaging Systems, *Proc. ACSM-ASPRS Annual Conference*, April 19-26, CD ROM.
- Toth C. K. and Grejner-Brzezinska D. A. 2001. Modern Mobile Mapping: Moving Toward GPS/INS-aided Real-time Image Processing, *Proceedings, ION GPS*, Salt Lake City, September 11-14, CD ROM.
- Toth Ch.K. and Csanyi N. 2001: Automating the LIDAR Bore-sight Misalignment, *ISPRS WGII/2 Workshop on Three-Dimensional Mapping from InSAR and LIDAR*, Banff, Alberta, Canada, 11-13 July, CD-ROM.
- Toth, C. 1998. Airborne Experiences with a 4K by 4K CCD Sensor, *Proc. ASPRS Annual Convention*, CD-ROM, pp. 163-168.
- Tu, Z., and R. Li, 2002. A Framework for Automatic Recognition of Spatial Features from Mobile Imagery. *Photogrammetric Engineering and Remote Sensing*, (683), pp.267-276.
- Wang J., L. Dai, T. Tsujii, C. Rizos, Grejner-Brzezinska D. A., Toth C. K. 2001. GPS/INS/Pseudolite Integration: Concepts, Simulation and Testing, *Proceedings, ION GPS*, Salt Lake City, September 11-14, CD ROM.